Catalyst–Substrate Adducts in Asymmetric Catalytic Hydrogenation. Crystal and Molecular Structure of [((*R*,*R*)-1,2-Bis{phenyl-*o*-anisoylphosphino}ethane)(methyl (*Z*)-β-propyl-α-acetamidoacrylate)]rhodium Tetrafluoroborate, [Rh(DIPAMP)(MPAA)]BF_4

Beth McCulloch and Jack Halpern*

Department of Chemistry, The University of Chicago, Chicago, Illinois 60637

Michael R. Thompson

Monsanto Company, St. Louis, Missouri 63167

Clark R. Landis*

Department of Chemistry and Biochemistry, University of Colorado, Boulder, Colorado 80309

Received July 27, 1989

[Rh(*R*,*R*-DIPAMP)$(MeOH)_2$]$^+$ (DIPAMP = 1,2-bis(phenyl-*o*-anisoylphosphino)ethane), which serves as an asymmetric hydrogenation catalyst for enamides, reacts with methyl (*Z*)-β-propyl-α-acetamidoacrylate (MPAA) to form the 1:1 adduct, [Rh(*R*,*R*-DIPAMP)(MPAA)]$^+$ (1), with a binding constant of 1.4×10^4 M^{-1} at 25 °C. Crystals of the BF_4 salt of the predominant diastereomer of 1 were isolated and subjected to single-crystal X-ray analysis. The structure of 1 resembles those deduced previously for rhodium [(1,2-bis(diphenylphosphino)ethane)(methyl(*Z*)-α-acetamidocinnamate)]tetrafluoroborate and rhodium [(2*S*,3*S*)-2,3-bis(diphenylphosphino)butane)(ethyl (*Z*)-α-acetamidocinnamate)] perchlorate. In this case also the face of the C=C bond (pro-*R*) that is coordinated to the Rh atom is opposite to that to which H_2 adds to form the predominant (*S*) enantiomer of the hydrogenated product. Accordingly, it is concluded that the origin of enantioselection in the [Rh(*R*,*R*-DIPAMP)]$^+$-catalyzed hydrogenation of MPAA is not the preferred mode of binding of the prochiral substrate but, rather, the higher reactivity toward H_2 of the minor, less stable, diastereomer of 1. The structural features of 1 that may be relevant to enantioselection are discussed.

Introduction

This paper extends our studies on the mechanisms and the origin of enantioselection in asymmetric catalytic hydrogenation.[1,2]

Prior investigations of this theme have focused on the hydrogenations of methyl and ethyl (*Z*)-α-acetamidocinnamates (MAC and EAC, respectively), catalyzed by rhodium(I) complexes of the chiral chelating diphosphine ligands 2,3-bis(diphenylphosphino)butane (CHIRAPHOS) and 1,2-bis(phenyl-*o*-anisoylphosphsino)ethane (DIPAMP).[1,3,4] A significant result was the finding that the enantioselection in these systems had its origin, not in the preferred mode of binding of the prochiral substrate to the chiral (diphosphine)rhodium(I) catalyst but, rather, in the higher reactivity toward oxidative addition of H_2 of the minor, less stable, diastereomer of the catalyst–substrate adduct. This conclusion was based on spectroscopic[3] and kinetic studies[2] and, in one case, [Rh(*S*,*S*-CHIRAPHOS)(EAC)]$^+$, determination of the absolute configuration of the major diastereomer of the catalyst–substrate adduct by X-ray crystallography.[4]

The remarkable enantioselectivities of these systems almost certainly have their origins in the steric features of the catalytic intermediates. Accordingly, it clearly is of interest to extend structural studies to other catalyst–substrate adducts. The present paper describes the synthesis and structural characterization, including X-ray structural analysis, of another such adduct, [Rh(*R*,*R*-DIPAMP)(MPAA)]$^+$ (MPAA = methyl (*Z*)-α-acetamido-β-propylacrylate). This system is of particular interest because (a) it constitutes the first X-ray structural elucidation of an eneamide adduct of [Rh(DIPAMP)]$^+$ and just the second crystal structure of an actual intermediate in the asymmetric hydrogenation catalytic cycle and (b) in contrast to the corresponding cinnamates such as MAC and EAC, where high enantioselectivities are obtained only with the *Z* isomers, hydrogenation with [Rh(*R*,*R*-DIPAMP)]$^+$ yields high enantiomeric excesses (in each case >95% *S* product) for both *Z*- and *E*-MPAA.[5]

Experimental Section

General Procedures. The general procedures were the same as those described previously for [Rh(*R*,*R*-DIPAMP)(MAC)]$^+$.[2] All reactions were performed under dry N_2 using standard Schlenck techniques. Solvents were distilled from appropriate drying agents and degassed by three freeze–pump–thaw cycles. ^1H NMR spectra were recorded on the University of Chicago Chemistry Department 500-MHz spectrometer and ^{31}P NMR spectra on a Nicolet 200 spectrometer at 80.988 37 MHz.

Synthesis of [Rh(*R*,*R*-DIPAMP)(MPAA)]$^+$[BF_4]$^-$ (1). [Rh(*R*,*R*-DIPAMP)$(MeOH)_2$]$^+$[BF_4]$^-$ was prepared as described earlier[2] by stirring a methanol solution of [Rh(*R*,*R*-DIPAMP)(norbornadiene)]$^+$[BF_4]$^-$ under H_2 until the color of the solution changed from red to yellow. H_2 was pumped off and a slight molar

(1) For leading references see: Halpern, J. In *Asymmetric Synthesis*; Morrison, J. D., Ed.; Academic Press: New York, 1985; Vol. 5, p 41, and references therein.
(2) Landis, C. R.; Halpern, J. *J. Am. Chem. Soc.* **1987**, *109*, 1746.
(3) Brown, J. M.; Chaloner, P. A. *J. Chem. Soc., Chem. Commun.* **1980**, 344.
(4) (a) Chan, A. S. C.; Pluth, J. J.; Halpern, J. *J. Am. Chem. Soc.* **1980**, *102*, 5952. (b) Chua, P. S.; Roberts, N. K.; Bosnich, B.; Okrasinski, S. J.; Halpern, J. *J. Chem. Soc., Chem. Commun.* **1981**, 1278.
(5) Scott, J. W.; Keith, D. D.; Nix, Jr., G.; Parrish, D. R.; Remington, S.; Roth, G. P.; Townsend, J. M.; Valentine, Jr., D.; Young, R. *J. Org. Chem.* **1981**, *46*, 5086.

0276-7333/90/2309-1392$02.50/0

Table I. Crystallographic Data

Crystals
color: translucent yellow needles
solvt syst: (CH_2Cl_2)
shape: needle
dimens: 0.10 × 0.10 × 0.15 mm
mount: glass fiber (0.15 mm, glue)
Instrumentation
diffractometer: Rigaku AFC-5
power settings: 50 kV × 180 (9.0 kW)
radiation: graphite-monochromated Cu Kα (λ = 1.5418 Å)
software: SDP/UCLA Crystallographic Software Package
computer: DEC VAX-8650
Crystal Class, Lattice Constants
crystal class: orthorhombic, space group $P2_12_12_1$ (No. 19)[a]
point group: D_2^4, lane symmetry 222
a = 15.366 (2) Å, b = 26.255 (4) Å, c = 10.234 (2) Å
α = 90.00, β = 90.00, γ = 90.00°
vol 4129 (2) Å^3, Z = 4, μ = 46.29
ρ_{calc} = 1.300 gm/cm^3, ρ_{measd} = not measured
Data Collection
scan type: $\theta/2\theta$, background 1.0-s peak scan time
scan width: 1.0° either side of the Kα doublet
no. of shells: three, 3.0–80, 80–100, 100–128°
scan speed: 2.0–6.0 (variable) deg/min
standards: 3 every 100, no deterioation and/or misalignment
total no. of reflns: 3862
no. of unique reflns = 3796
no. of obsd reflns = 2417
rejection criterion = 3.0($\sigma(I)$)

[a] "International Tables for X-ray Crystallograpy"; Kynoch Press: Birmingham, England, 1969; Vol. I; p. 105.

excess of MPAA was added. X-ray quality crystals of [Rh(*R*,*R*-DIPAMP)(MPAA)]$^+$[BF_4]$^-$ were obtained by recrystallization from methanol. In methanol, only one diastereomer could be detected by NMR. $^{31}P\{^1H\}$ NMR δ 69.6 (dd, 1 P, P_1, J_{Rh-P_1} = 163 Hz), 45.6 (dd, 1 P, P_2, J_{Rh-P_2} = 155 Hz, $J_{P_1-P_2}$ = 40 Hz) (closely resembling that reported previously for the major diastereomer of [Rh(*R*,*R*-DIPAMP)(MAC)]$^+$).[2]

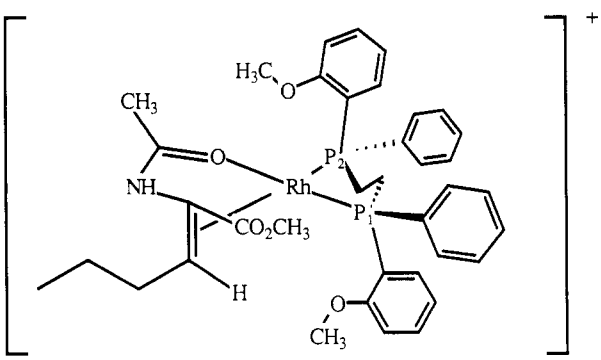

(1)

The equilibrium constant for binding of MPAA to [Rh(*R*,*R*-DIPAMP)]$^+$ at 25 °C in methanol (eq 1) was determined by spectral titration as described earler[2] to be 1.4 × 10^4 M^{-1} (vs 3.5 × 10^4 M^{-1} for the major diastereomer of [Rh(*R*,*R*-DIPAMP)-(MAC)]$^+$).

$$[Rh(R,R\text{-DIPAMP})(MeOH)_2]^+ + MPAA \rightleftharpoons [Rh(R,R\text{-DIPAMP})(MPAA)]^+ \quad (1)$$

Crystallographic Data Collection, Reduction, Solution and Refinement. Crystallographic data are listed in Table I.

Crystals of **1** were insufficient in size for use in diffraction studies with a conventional low-power sealed-tube X-ray source. A 0.10 × 00.10 × 0.15 mm crystal was glued to the end of a thin glass fiber (0.07 mm), mounted, and optically aligned on a Rigaku AFC5 diffractometer equipped with a 12.0-kW rotating anode generator (power settings: 50 kV × 180 mA, 9.0 kW) and a copper anode. Fifteen reflections with 2θ (Cu Kα) <40.0° were centered and a preliminary set of lattice constants determined. Reduction

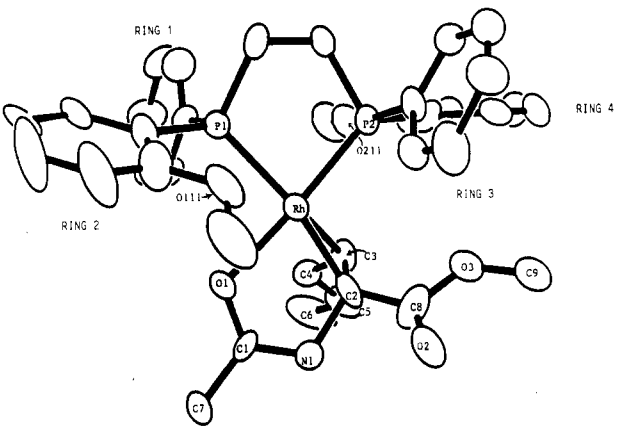

Figure 1. Structure of [Rh(*R*,*R*-DIPAMP)(MPAA)]$^+$.

of the cell resulted in an orthorhombic description with a = 15.366 (2) Å, b = 26.255 (4) Å, c = 10.234 (2) Å, V = 4129 (2) Å^3, Z = 4, density$_{calc}$ = 1.300 g/cm^3 and μ = 46.29 cm^{-1}. An intensity data set was collected in the $\theta/2\theta$ scan mode, with a 1.0° stepoff, and background count time equal to the total peaks accumulation time. Data were collected in four shells of increasing 2θ; 3.0–80.0°, 80.0–100°, and 100.0–128.0°. Three standard reflections were collected every 100 reflections as a monitor of crystal deterioration and/or misalignment (none detected). A total of 3796 independent reflections were collected, of which 1379 were rejected as objectively unobserved by applying a rejection criterion of $I > 3\sigma(I)$. The remaining 2417 reflections were corrected for absorption effects by applying an empirical absorption correction (ψ scans) and reduced to the relative squared amplitudes by means of standard Lorentz and polarization corrections.

The coordinates for the rhodium atom were deduced from a Patterson synthesis[6] and included in initial cycles of isotropic full-matrix least-squares refinement, resulting in conventional residuals R_1 (unweighted, based on F)[7,8] = 0.398 and R_w (weighted, based on F) = 0.391 for 2417 reflections. The phosphorus coordinates were deduced from a difference Fourier map calculated by using the phases calculated from the one-atom model. Isotropic least-squares refinement of these three atoms resulted in residuals R_1 = 0.354 and R_w = 0.361. The remaining 48 non-hydrogen atoms contained in the asymmetric unit were located in a subsequent difference Fourier and included in isotropic full-matrix least-squares refinement, converging at R_1 = 0.135 and R_w = 0.140 for the 2417 reflections. All 51 non-hydrogen atoms comprising the Rh-centered cation and BF_4 anion were given anisotropic thermal factors and further refined by means of full-matrix least-squares analysis, resulting in R_1 = 0.086 and R_w = 0.088. Large errors and elongated thermal elipses were noted for the fluorine atoms of the anion, attributable to high thermal motion, disorder, and absorption effects. No solvate molecules could be located in the lattice. Hydrogen atoms were included in subsequent cycles of refinement, either generated in idealized geometry (C–H distance 1.0 Å) where possible or located via difference Fourier for terminal CH_3. Final cycles of least-squares refinement utilized a σ-weighting scheme ($1/\sigma(F\sigma)$) and resulted in final convergence at R_1 = 0.061 and R_w = 0.061 for 2417 reflections and σ = 2.73.

The coordinates for this enantiomorph were inverted and refined in order to determine the absolute configuration. Convergence resulted at residuals 1% higher: R_1 = 0.071 and R_w = 0.073 for the 2417 reflections.

(6) *Structure Determination Package*; B. A. Frenz Associates, Inc., College Station, TX, and Enraf-Nonius, Delft, Holland. Calculations performed on a DEC VAX-8650; *The UCLA Crystallographic Package*; Department of Chemistry, University of California, Los Angeles, CA 90024.

(7) The R values are defined as $R_1 = \sum||F_o| - |F_c||/\sum|F_o|$ and $R_w = |\sum w(F_o - |F_c|)^2/\sum w|F_o|^2|^{1/2}$, where w is the weight given each reflection. The function minimized is $\sum w(|F_o| - K|F_c|)^2$, where K is the scale factor. Weights are defined as $W = 1/\sigma^2(F_o)$.

(8) Versions of programs ORFLS (Busing, Martin and Levy), ORFFE (Busing, Martin and Levy), HYDROGEN (Trueblood), ORTEP (Johnson). All calculations were performed on a DEC VAX 8650.

Table II. Atomic Fractional Coordinates[a,b]

atom	x	y	z	B(iso), Å²
Rh	0.0470 (1)	0.6100 (1)	0.5408 (1)	601 (8)
P1	0.0618 (4)	0.6940 (2)	0.5895 (5)	66 (4)
P2	0.0173 (3)	0.6400 (2)	0.3409 (5)	62 (4)
N1	0.0499 (18)	0.5100 (6)	0.6640 (17)	85 (14)
O1	0.0876 (10)	0.5873 (5)	0.7287 (12)	80 (11)
O2	0.1101 (13)	0.4733 (7)	0.4322 (16)	127 (16)
O3	0.0034 (12)	0.5069 (6)	0.3202 (15)	97 (13)
O111	0.2267 (12)	0.6421 (8)	0.5702 (15)	115 (15)
O211	-0.1603 (11)	0.6556 (7)	0.4239 (16)	101 (14)
C1	0.0819 (19)	0.5404 (8)	0.7526 (23)	91 (19)
C2	0.0155 (14)	0.5363 (9)	0.5426 (21)	84 (16)
C3	-0.0564 (12)	0.5607 (7)	0.5418 (20)	63 (12)
C4	-0.1165 (14)	0.5646 (7)	0.6491 (21)	73 (15)
C5	-0.1957 (18)	0.5294 (11)	0.6405 (25)	119 (24)
C6	-0.2608 (20)	0.5352 (12)	0.7400 (28)	171 (32)
C7	0.1154 (21)	0.5186 (9)	0.8792 (20)	124 (23)
C8	0.0469 (20)	0.5018 (9)	0.4384 (32)	108 (21)
C9	0.0335 (20)	0.4777 (9)	0.2112 (22)	118 (23)
C10	0.0725 (14)	0.7304 (8)	0.4377 (20)	77 (16)
C11	0.0089 (14)	0.7091 (8)	0.3419 (18)	72 (15)
C111	0.1578 (18)	0.7097 (10)	0.6816 (23)	90 (20)
C112	0.2363 (18)	0.6789 (12)	0.6591 (27)	100 (23)
C113	0.3051 (19)	0.6896 (15)	0.7258 (28)	148 (31)
C114	0.3198 (27)	0.7243 (19)	0.8064 (41)	213 (50)
C115	0.2360 (30)	0.7563 (12)	0.8359 (30)	155 (33)
C116	0.1561 (22)	0.7490 (10)	0.7792 (25)	130 (25)
C117	0.2954 (19)	0.6055 (16)	0.5782 (27)	178 (32)
C121	-0.0270 (15)	0.7178 (8)	0.6779 (24)	75 (17)
C122	-0.0684 (21)	0.7612 (10)	0.6483 (24)	115 (23)
C123	-0.1443 (27)	0.7789 (10)	0.7081 (30)	140 (30)
C124	-0.1723 (22)	0.7504 (13)	0.8058 (35)	132 (31)
C125	-0.1319 (21)	0.7082 (10)	0.8440 (24)	115 (23)
C126	-0.0616 (20)	0.6915 (8)	0.7811 (25)	100 (21)
C211	-0.0731 (14)	0.6223 (8)	0.2545 (24)	76 (17)
C212	-0.1589 (17)	0.6326 (9)	0.3037 (25)	82 (18)
C213	-0.2334 (18)	0.6195 (11)	0.2431 (27)	105 (23)
C214	-0.2246 (19)	0.5954 (10)	0.1178 (29)	110 (24)
C215	-0.1406 (19)	0.5838 (10)	0.0682 (23)	96 (20)
C216	-0.0676 (17)	0.5975 (9)	0.1307 (23)	93 (20)
C217	-0.2441 (16)	0.6672 (12)	0.4810 (27)	130 (24)
C221	0.1072 (12)	0.6281 (8)	0.2288 (19)	56 (13)
C222	0.1102 (16)	0.6540 (8)	0.1105 (21)	87 (18)
C223	0.1818 (17)	0.6434 (9)	0.0319 (26)	98 (20)
C224	0.2494 (15)	0.6131 (11)	0.0653 (26)	98 (20)
C225	0.2444 (15)	0.5839 (11)	0.1834 (25)	109 (21)
C226	0.1739 (17)	0.5967 (9)	0.2588 (21)	87 (19)
B	0.0507 (41)	0.8930 (33)	0.6394 (161)	419 (125)
F1	-0.4338 (14)	0.6442 (7)	0.3442 (30)	220 (23)
F2	0.0737 (15)	0.9366 (7)	0.6052 (26)	226 (25)
F3	-0.0269 (26)	0.9073 (8)	0.7167 (41)	291 (33)
F4	-0.0135 (24)	0.8905 (16)	0.5276 (33)	296 (34)

[a] Atoms are labeled in accordance with Figure 1. Numbers in parentheses are the estimated standard deviations in the least significant figure. [b] The form of the equivalent isotropic temperature is $^4/_3[a^2B(1,1) + b^2B(2,2) + c^2B(3,3) + ab(\cos\gamma)B(1,2) + ac(\cos\beta)B(1,3) + bc(\cos\alpha)B(2,3)]$.

Results and Discussion

The results of the X-ray crystal structure determination of 1 are listed in Tables II–VI (Tables IV–VI are in the supplementary material; see the paragraph at the end of the paper). The structure of $[Rh(DIPAMP)(MPAA)]^+$ is depicted in Figure 1.

The coordination environment of the Rh atom in the $[Rh(DIPAMP)(MPAA)]^+$ ion, depicted in Figure 1, is similar to those of the crystallographically characterized enamide complexes, $[Rh(DIPHOS)(MAC)](BF_4)$[3] and $[Rh(CHIRAPHOS)(EAC)](ClO_4)$.[4] As in the latter structures, the prochiral enamide is coordinated to the Rh atom through the oxygen atom of the enamide carbonyl and through symmetrical (η^2) coordination of the C–C double bond. Together with the normal chelation of the DIPAMP ligand, the overall coordination around the Rh atom approximates an idealized square-planar arrangement of ligands (C–C, O, 2P). Bond angles and bond lengths about the Rh atom are similar to those of the other crystallographically characterized enamide complexes.

Table III. Selected Bond Lengths (Å) and Bond Angles (deg)[a]

Rh-P1	2.272 (6)	C2-C3	1.227 (24)
Rh-P2	2.239 (6)	P1-C121	1.752 (24)
Rh-O1	2.108 (13)	P1-C111	1.798 (24)
Rh-C2	1.995 (24)	P1-C10	1.831 (20)
Rh-C3	2.049 (18)	P2-C211	1.711 (22)
N1-C1	1.304 (2)	P2-C221	1.823 (19)
N1-C2	1.517 (26)	P2-C11	1.819 (21)
C1-O1	1.258 (21)	C1-C7	1.507 (28)
C2-C8	1.480 (35)	C3-C4	1.438 (26)
C2-Rh-O1	77.8 (7)	C2-Rh-P2	107.5 (6)
C2-Rh-P1	164.5 (7)	C3-Rh-O1	92.7 (7)
C3-Rh-P2	93.9 (6)	C3-Rh-P1	133.6 (6)
O1-Rh-P2	173.4 (5)	O1-Rh-P1	92.6 (4)
P2-Rh-P1	83.1 (2)	C1-N1-C2	115.0 (17)
C3-C2-C8	125.8 (24)	C3-C2-N1	122.4 (23)

[a] Atoms are labeled in accordance with Figure 1. Numbers in parentheses are the estimated standard deviations in the least significant figure.

The chirality of the olefin–rhodium binding is such that, assuming cis-endo hydrogen transfer,[10] the chirality of the methyl α-acetamidobutanoate product would be *R*. However, the predominant chirality of the product of the catalytic hydrogenation reaction is *S* (>95% enantiomeric excess). Thus it would appear that, as previously found for $[Rh(CHIRAPHOS)(EAC)](ClO_4)$, the diastereomer of $[Rh(DIPAMP)(MPAA)](BF_4)$ which crystallizes from solution contributes little to product formation. Extrapolation from a large body of accumulated evidence supports the identification of the crystallized (pro-*R*) diastereomer as the more stable, major, diastereomer in solution. The reactivity of this diastereomer toward H_2 apparently is much lower than that of the minor, less stable, pro-*S*, diastereomer so that the predominant product enantiomer (*S*) derives from the latter.

Considering the paucity of established structures for prochiral substrates bound to chiral hydrogenation catalysts, a few additional comments on the structural features of $[Rh(DIPAMP)(MPAA)](BF_4)$ are warranted. A more complete analysis of experimental and computational structural features and their relevance to the origins of enantioselection is forthcoming by one of us (C.R.L.).

It is observed that catalysts containing chiral sites quite remote (e.g., CHIRAPHOS) from the actual sites of substrate attachment nevertheless can effect nearly quantitative enantioselection. Two prominent, but compatible, views concerning the mode of transmission of chirality from a remote site emphasize the influence of the remote site on the orientations of the arene rings attached to the phosphorus atoms. Knowles et al.[11] have focused on the tendency of the arene rings to adopt chiral, alternating

(9) Chan, A. S. C.; Pluth, J. J.; Halpern, J. *Inorg. Chim. Acta* **1979**, *37*, L477.

(10) A referee has pointed out that cis transfer has been demonstrated for the hydrogenation of prochiral enamides catalyzed by $Rh(PPh_3)_3Cl$. Kirby, G. W.; Michael, J. *J. Chem. Soc., Perkin Trans. 1* **1973**, 115.

(11) (a) Vineyard, B. D.; Knowles, W. S.; Sabacky, M. J.; Backman, G. L.; Weinkauff, D. G. *J. Am. Chem. Soc.* **1977**, *99*, 5946. (b) Knowles, W. S.; Vineyard, B. D.; Sabacky, J. J.; Stults, B. R. In *Fundamental Research in Homogeneous Catalysis*; Plenum Press: New York, 1979; Vol. 3, p 537. (c) Koenig, K. E.; Sabacky, M. J.; Backman, G. L.; Christopfel, W. C.; Barnstorff, H. D.; Friedman, R. B.; Knowles, W. S.; Stults, B. R.; Vineyard, B. D.; Weinkauff, D. J. *Ann. N.Y. Acad. Sci.* **1980**, *333*, 16.

edge–face–edge–face orientations with the bulkier anisoyl rings preferring the "facial" orientation. Bosnich et al.,[12] on the basis of their investigations of the effect of varying ring size on ring conformational preferences, have stressed the chirality inherent in the quasi-equatorial and -axial dispositions of the arene rings. Recently, Brown and Evans[13] have extended the analysis of arene torsion angles originally reported by Oliver and Riley[14] to a broad range of crystallographically characterized complexes containing chiral diphosphines.

The structure of [Rh(DIPAMP)(MPAA)](BF_4) demonstrates arene ring conformations similar to those of [Rh(DIPAMP)(1,5-cyclooctadiene](BF_4).[11c] Using the conventions of Brown and Evans, the normalized arene ring torsion angle values (θ and ϕ for each ring) of 1 are $\theta = 45°$, $\phi = 105°$; $\theta = 52°$, $\phi = 133°$; $\theta = 12°$, $\phi = 107°$; $\theta = 61°$, $\phi = 129°$ for rings 1–4, respectively. (Values for [Rh(DIPAMP)(1,5-cyclooctadiene](BF_4) are $\theta = 3°$, $\phi = 104°$; $\theta = 75°$, $\phi = 137°$; $\theta = 23°$, $\phi = 98°$; $\theta = 66°$, $\phi = 140°$). Idealized edge–face arene ring arrays as defined by Brown and Evans correspond to $\theta = 0°$ (edge) and $\theta = 70°$ (face); axial groups have $\phi \simeq 100°$ and equatorial groups have $\phi \simeq 130°$. It should be noted that the closest interaction between an axial arene ring and a ligand in the cis-coordination site of the square plane does not occur at $\theta = 0°$ but, rather, occurs in the range $\theta \simeq 30$–$40°$. Arene rings 3 and 4, which are cis to the C=C of the enamide, display a nearly ideal edge–face orientation, whereas the rings 1 and 2 conform less well to this idealized structure.

The oxygen atoms of *o*-anisoylphosphines can coordinate to metals, forming chelate rings. Indeed, such coordination has been invoked to explain the enhanced nucleophilicity of *o*-anisoylphosphine, relative to *p*-anisoylphosphine, analogues of Vaska's complex toward CH_3I[15] and has been observed by Brown and Maddox[16] for alkylhydridoiridium complexes containing the DIPAMP ligand. For [Rh(DIPAMP)(MPAA)](BF_4) the Rh–O distances for the anisoyl oxygens (Rh–O1111 = 2.903 Å, Rh–O211 = 3.607 Å) are sufficiently longer than normal Rh–O bonding distances (Rh–O = 2.1 Å) that normal bonding interactions are excluded, although weak interactions may be important. Additionally, agostic interactions involving ortho hydrogens of the diphosphine axial arene rings have been proposed;[13] addition of hydrogen atoms to the *o*-arene carbon atoms at normal bond lengths yields Rh–H(ortho) distances of 2.9 and 3.3 Å. The axial arene rings display smaller Rh–P–C(arene) bond angles (112 and 111°) than the equatorial arene rings (115 and 122°), which is not inconsistent with the possibility of an agostic interaction.

Acknowledgment. We are grateful to the National Science Foundation (J.H.) and to the National Institutes of Health (C.R.L.) for grants in support of this research, to Johnson Matthey Inc. for a generous loan of rhodium trichloride, and to Dr. J. W. Scott of Hoffman-LaRoche Inc. for a generous gift of MPAA.

Supplementary Material Available: Listings of H atom coordinates and anisotropic thermal parameters (Tables IV and V) (2 pages); a listing of structure factors (8 pages). Ordering information is given on any current masthead page.

(12) Bosnich, B.; Roberts, N. K. *Adv. Chem. Ser.* **1982**, *196*, 337, and references therein.
(13) Brown, J. M.; Evans, P. L. *Tetrahedron* **1988**, *44*, 4905.
(14) Oliver, J. D.; Riley, D. P. *Organometallics* **1983**, *2*, 1032.
(15) Miller, E. M.; Shaw, B. L. *J. Chem. Soc., Dalton Trans.* **1974**, 480.
(16) Brown, J. M.; Maddox, P. J. *J. Chem. Soc., Chem. Commun.* **1987**, 1276.

Stabilization of the First Selenogermylene as the Monomeric Pentacarbonyltungsten(0) Complex

Wolf-W. du Mont,* Lutz Lange, Siegfried Pohl, and Wolfgang Saak

Fachbereich Chemie der Universität Oldenburg, P.O. Box 2503, D-2900 Oldenburg, Federal Republic of Germany

Received August 4, 1989

Bis[(2,4,6-tri-*tert*-butylphenyl)seleno]germylene, formed in situ by reaction of lithium 2,4,6-tri-*tert*-butylphenyl selenide with the germanium dichloride dioxane complex, was trapped as the monomeric pentacarbonyl[bis((2,4,6-tri-*tert*-butylphenyl)seleno)germylene]tungsten(0) complex. Reaction of bis(2,4,6-tri-*tert*-butylphenyl) diselenide with the germanium dichloride dioxane complex provides dichlorobis((2,4,6-tri-*tert*-butylphenyl)seleno)germane. This tetravalent germanium compound and bis(2,4,6-tri-*tert*-butylphenyl) diselenide were identified as byproducts when preparation and isolation of the monomeric selenogermylene was attempted. The structure of the selenogermylene tungsten(0) complex was determined from single-crystal X-ray diffraction data. The complex crystallizes (with one toluene per molecule) in the monoclinic space group $P2_1/c$ with $a = 1077.4$ (2), $b = 1667.2$ (2), $c = 2880.9$ (2) pm, $\beta = 98.33°$, and $Z = 4$. The molecule contains trigonal planar germanium with bonds to tungsten and to two nonequivalent selenium atoms (Ge–Se, 231.4 (2) and 234.6 (2) pm; Ge–W, 252.8 (1) pm). Well-resolved ^1H, ^{13}C, and ^{77}Se NMR signals for the two (2,4,6-tri-*tert*-butylphenyl)seleno groups of the selenogermylene complex indicate hindered rotation around the Ge–Se bonds at room temperature in solution.

Introduction

Carbene-analogous germylenes are known with C, N, O, P, and S atoms bonded to divalent germanium, but a monomeric germylene with a post-transition element like As or Se adjacent to germanium has not yet been characterized.[1] Low molecular weight compounds with covalent bonds between unsaturated germanium and soft and easily polarizable selenium atoms would be of interest as

(1) For the synthesis of *t*-$Bu_2AsGeCl$ and *t*-$Bu_2AsSnCl$ see: du Mont, W.-W.; Rudolph, G. *Z. Naturforsch.* **1981**, *36B*, 1215. Cowley, A. H.; Giolando, D. M.; Jones, R. A.; Nunn, C. M.; Power, J. M.; du Mont, W.-W. *Polyhedron* **1988**, *7*, 1317.

0276-7333/90/2309-1395$02.50/0